Sequestration of toxic Congo red dye through the utilization of red dragon fruit peel: linear versus nonlinear regression analyses of isotherm and kinetics

Linda B.L. Lim[a,*], Namal Priyantha[b,c], Siti Amanina Abdul Latip[a], YieChen Lu[a]

[a]*Department of Chemistry, Faculty of Science, Universiti Brunei Darussalam, Jalan Tungku Link, Gadong,*
Negara Brunei Darussalam, Tel. 00-673-8748010; emails: linda.lim@ubd.edu.bn (L.B.L. Lim),
nyna.al611@gmail.com (S.A.A. Latip), yiechen_93@hotmail.com (Y.C. Lu)
[b]*Department of Chemistry, Faculty of Science, University of Peradeniya, Peradeniya, Sri Lanka,*
email: namal.priyantha@yahoo.com
[c]*Postgraduate Institute of Science, University of Peradeniya, Peradeniya, Sri Lanka*

ABSTRACT

The adsorption system of toxic Congo red (CR) industrial dye and red dragon fruit peel (RDFP), a low-cost natural adsorbent reached equilibrium within half an hour. The adsorbent shows high stability and is reasonably resilient to changes in pH while exhibiting strong adsorption characteristics toward CR in solutions of varying ionic strength. The isotherm model among Langmuir, Freundlich, Temkin, Redlich–Peterson and Sips evaluated based on R^2, five error functions together with Akaike information criterion indicates that the Sips model is the best fit with the maximum adsorption capacity (q_{max}) of 71.74 mg g^{-1}, even though the nonlinear regression suggests that the Redlich–Peterson model followed by the Sips model be more suitable to describe the adsorption process. Moreover, there is no statistical difference between linear and nonlinear regression methods, implying that the Sips model is the most appropriate to describe the adsorption system under investigation. Kinetics of interaction of CR and RDFP can be best described by the pseudo-second-order model with the rate constant of 3.82 g mmol^{-1} min^{-1}. When compared to many reported adsorbents, RDFP exhibits much higher q_{max}. All the above results indicate that RDFP has the potential in its application as a good candidate for the removal of CR dye in wastewater treatment.

Keywords: Red dragon fruit peel; Pitaya; *Hylocereus polyrhizus*; Adsorption isotherm; Congo red; Azo dye; Kinetics; Nonlinear regression

1. Introduction

The fast-growing world's population has led to the rise in food industries and boom in fast-food restaurants and chains in order to cater to the needs of the people. This comes at a price for it is well known that consumption of too much-processed food and an unhealthy diet has led to many health problems. Today, amongst the many diseases, cardiovascular diseases and cancer are the two major causes of death. As a means of reducing the risk of these diseases, the World Health Organization (WHO) has recommended the consumption of at least 400 g of fruits and vegetables per day. Fruits are a rich source of vitamins, minerals, essential nutrients and antioxidants. With more people becoming aware of the health benefits of fruits [1], the global production of fruits has increased. Unavailability of certain fruits throughout the year and their relatively short shelf life has led to fruits being processed. As a result, it is inevitable that the by-products of fruits such as peels, core, seeds, which are normally inedible and thrown away as wastes, are also on the rise. Some fruits, such as *Artocarpus odoratissimus* contain more than 50% inedible

* Corresponding author.

parts, of which the peel contributes the major portion [2]. These agro-wastes not only contribute to the landfill but if untreated can cause serious environmental pollution problems. Hence, attempts to convert them into useful material have been researched upon. One such area of research is the utilization of fruit waste as natural low-cost adsorbents for the removal of heavy metals [3–6] and dyes [7–13]. The most desirable factor of this process would be the conversion of unwanted waste into economical material to be used in wastewater treatment to reduce environmental pollution.

One of the exotic fruits which have gained popularity in recent years is the *Hylocereus polyrhizus* of the Cactaceae family. *Hylocereus polyrhizus* is otherwise known as pitaya or red dragon fruit. Its origins were from tropical and subtropical America although it has been widely cultivated in many Asian countries. It is considered a super-food packed with vitamins, minerals, antioxidants, etc. [14–16]. Research has shown that dragon fruit has anti-cancer properties, and it has the ability to reduce prostate and colorectal cancer as well as promote healthy gut flora [17].

Recent studies have shown that red dragon fruit is not only beneficial to health, red dragon fruit peel (RDFP) is also rich in vitamins and minerals [18]. The presence of betacyanins allows the RDFP to be used as a natural dye in food [19]. The study has also indicated that the chloroform extract of RDFP exhibited antibacterial activity where inhibition of almost all the pathogens studied was observed [20]. Compounds isolated from the RDFP were also found to have the ability to flex the blood vessels. Research carried out with male BALB/c mice showed that RDFP can improve the blood lipid levels of hyperlipidemia in these mice [21].

Nevertheless, since not all the RDFP are being utilized, they are often disposed as waste. The presence of various compounds in the peel could provide functional groups that could facilitate the adsorption of pollutants. In fact, previous studies have shown that RDFP was able to remove heavy metals, such as Mn(II), Cd(II), Pb(II), and Ni(II) [22–24]. It has also been found to have the ability to remove dyes, such as Methylene blue, Alcian blue, Coomassie brilliant blue G-250 and Neutral red [24–26]. However, its use for the removal of anionic dyes has not been previously reported, to the best of our knowledge. Hence, in order to evaluate the possibility of using RDFP as an adsorbent to remove anionic dye, Congo red (CR) was chosen in this study to be the model dye. CR, whose structure is as shown in Fig. S1, is a diazo dye with a benzidine based structure. CR is the first direct dye that enables dyeing of cotton without the presence of dye fixative [27]. Apart from its use as a dye in the textile industry, the detection of amyloids is possible in histological staining using CR dye as a means of diagnosing amyloidosis diseases [28]. CR being structurally stable is not an easily biodegradable dye, although nanomaterials have been used to degrade this dye [29,30]. Despite its uses, CR is known to be toxic with carcinogenic effects [31,32]. Studies have shown that occupational exposure to benzidine based dye resulted in bladder tumor [33]. Further, it was found that prenatal administration of CR to mice and rats reduced the number of germ cells in both the male and female offspring [34]. Therefore, given its toxicity and hazardous to health, its removal from wastewater is crucial.

Another aspect to be considered is that comparison between linear and nonlinear regression analysis for dye adsorption has not been well studied despite the need for extension of the methodology developed under static conditions for large-scale applications under dynamic conditions. In this context, this research mainly focused on a detailed investigation of adsorption equilibrium aspects of the CR-RDFP system with the aid of different adsorption isotherm model fittings, as well as on the adsorption kinetics using pseudo-order models through both linear and nonlinear regression analyses.

2. Methods

2.1. Preparation of adsorbent

Random samples of red dragon fruit (*Hylocereus polyrhizus*) were purchased from supermarkets in the Brunei-Muara District of Negara Brunei Darussalam. RDFP was separated from its edible flesh, cut into smaller pieces and dried in an oven at 60°C until a constant mass was obtained. The dried RDFP sample was then ground and sieved with a metal sieve apparatus to obtain particles of diameter <355 μm, and stored in sealed bags until ready to be used.

2.2. Selected adsorbate

Congo red (CR) dye ($C_{32}H_{22}N_6Na_2O_6S_2$, MW 696.66 g mol^{-1}), the adsorbate selected in this study, was purchased from Sigma-Aldrich, Singapore. The absorbance of CR in all solutions was measured using the Shimadzu UV-1601 PC UV-visible spectrophotometer (Japan), set at wavelength 500 nm.

2.3. Optimization of parameters and batch adsorption studies

Optimization of parameters in this study involved the investigation into the contact time required to reach equilibrium (0–210 min), effects of changing pH (4–12) and varying NaCl concentrations (0–1.0 M) using 100 mg L^{-1} CR dye solution. Adjustment of pH was done using either 1.0 M HCl and/or NaOH. Adsorption isotherm was carried out in different CR concentrations (0–1,000 mg L^{-1}), whilst 100 mg L^{-1} CR was used for kinetics studies. All experiments in this study were carried out with RDFP (0.020 g) in CR dye solution (10.0 mL), unless otherwise stated. The RDFP-CR suspensions were shaken at 250 rpm at room temperature.

3. Results and discussion

3.1. Functional groups and surface morphology of RDFP

The Fourier-transform infrared spectroscopy (FTIR) spectrum of RDFP, prior to its adsorption of CR dye, given in Fig. 1 shows the presence of many functional groups, namely, OH/NH (3,423 cm^{-1}), C=O (1,730 cm^{-1}), C=C (1,643 cm^{-1}), C–N (1,326 cm^{-1}) and aromatic skeletal vibrations (891 cm^{-1}). Further, peaks at 2,918 and 2,851 cm^{-1} are associated with vibrations of CH$_2$ and CH groups. The large shift observed for OH/NH group to 3,482 cm^{-1} upon the treatment of RDFP with CR dye indicates that these functional groups are very likely to be involved in the

adsorption process. Smaller shifts are also observed for C=O, C=C, C–N, and aromatic skeletal vibrations. There is also an intensification of peaks in the area between 1,000 to 1,108 cm⁻¹ region attributing to C–O stretching of alcohols and in-plane bending and skeleton vibrations of benzene ring [35,36], while the increase in the relative intensity of peak at 1,429 cm⁻¹ is attributed to N=N [37]. The asymmetry vibration of S=O stretch appears at 1,324 and 1,161 cm⁻¹ while symmetry S–O stretch is at 1,054 cm⁻¹ [38].

Images of scanning electron microscopy (SEM) in Fig. 2 show that the surface morphology of RDFP has undergone distinct changes upon adsorption of CR dye. RDFP, before adsorption, has a rough and irregular surface with some cavities in it. Interestingly, after adsorption of CR dye, its surface appears to be covered with dye and became less irregular with larger undulating folds across the whole surface. Similar observations were also reported for adsorption of CR onto white dragon fruit peel whereby the rough, undulating folded surface became smooth as a result of coverage of CR dye [39]. In fact, changes to surface morphology of adsorbents have been widely reported upon adsorption of dyes [40–42].
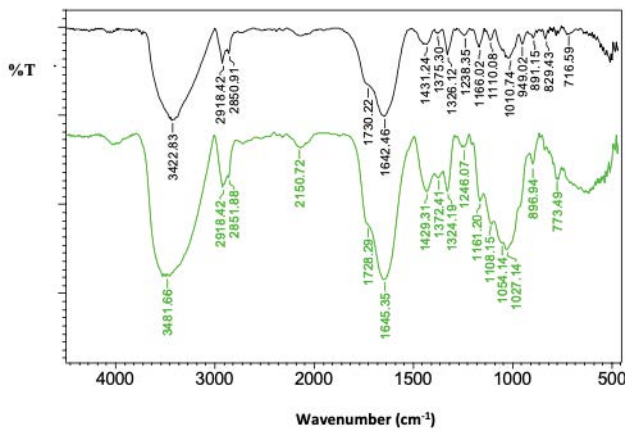
According to FTIR spectral characteristics and SEM images, it can be stated that both electrostatic interaction and deposition on pores of RDFP would contribute to the mass transfer process of CR dye. Initial layer of CR dye adsorbed on RDFP would be chemisorption, followed by physisorption of subsequent layers of CR dye molecules.

3.2. Effect of shaking time on adsorption of CR onto RDFP

In adsorption studies, it is imperative to conduct an investigation of the time required for an adsorbent-adsorbate system to reach equilibrium. This data is crucial for the design and operation of wastewater treatment plants. The adsorption of CR onto RDFP was rapid, reaching equilibrium within 30 min with more than 90% dye removal (Fig. 3). At the beginning stage of the adsorption process, many active binding sites on the surface of RDFP are vacant allowing CR dye molecules to be quickly adsorbed. However, as these sites are being filled, the rate of adsorption would decrease over time and gradually reach equilibrium. This is indicated by the plateau as the contact time increases, signifying that no more CR molecules are being adsorbed. A short period of contact time is always preferred since when applied to wastewater treatment it will translate as cost-saving, and therefore be more economical and profitable.
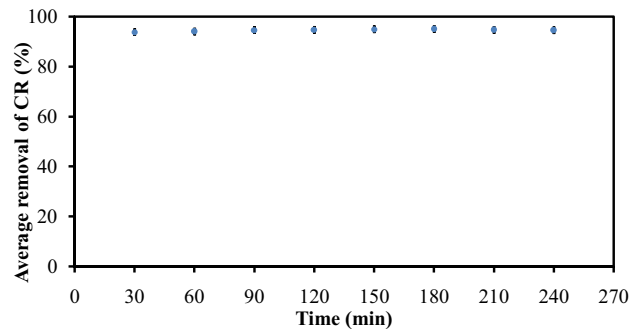

Fig. 1. FTIR spectra of RDFP before (black) and after (green) adsorption of CR dye.

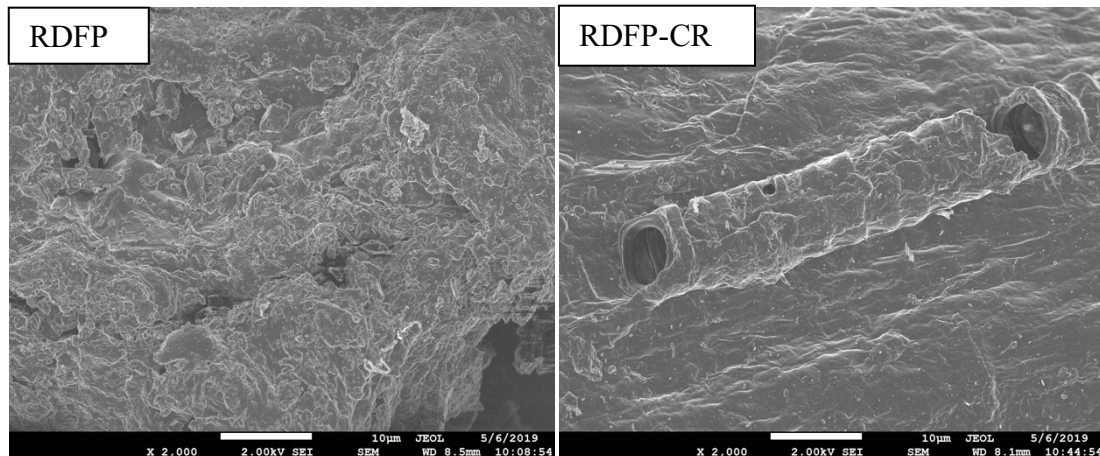Fig. 3. Effect of contact time on the adsorption of CR onto RDFP.

Fig. 2. SEM of RDFP before and after adsorption of CR dye at 2,000× magnification.

3.3. Effect of change in pH and presence of salts on adsorption of CR onto RDFP

For an adsorbent to be applicable in wastewater treatment, it has to be stable in the sense that it should be able to maintain relatively good adsorption ability under various environmental conditions such as changes in pH and ionic strength. This is because wastewater often contains various effluents and therefore is never at neutral pH or without the presence of electrolytes. These ions can interact with the adsorbent and/or adsorbate, thereby affecting the removal of the adsorbate.

In this study, an investigation of pH was carried out in the range of pH 4–12. It was observed that below pH 4, there was a change in the color of CR solution and hence, any results obtained at pH < 4 will be deemed inaccurate. Fig. 4a indicates that RDFP is relatively stable and resilient to changes in medium pH. The point of zero charge (pH_{pzc}) was determined at pH 7.4 following the method as outlined by Dahri et al. [43]. Below this pH, protonation of the surface functional groups would take place causing the surface of RDFP to be predominantly positively charged. Even though CR is an anionic dye, the presence of lone pairs of electrons on the amino groups could be attracted to the positively charged surface. At pH > pH_{pzc} of RDFP, deprotonation of surface functional groups would take place resulting in a predominantly negatively charged surface, promoting electrostatic repulsion between the RDFP and anionic CR dye molecules. Hence, this could explain the

observed decrease in the removal of CR at pH 10. However, the unexpected increase in the extent of removal of CR at pH = 12 could be due to a different mode of mass transfer, probably deposition of CR anionic dye in adsorbent pores which is not affected by surface charge.

As for the investigation of the influence of ionic strength on the adsorption of CR dye onto RDFP, NaCl was chosen because many dyeing industries often use sodium salts as the stimulator. Fig. 4b shows that the adsorbent performed better in the presence of NaCl, with enhanced removal over the range of concentrations studied. This could be due to screening effects of electrolytes thereby decreasing the repulsive forces among surface functional groups of RDFP, which in turn would enforce electrostatic interactions between RDFP and CR.

Since the stability of an adsorbent under various environmental changes is an important issue in wastewater treatment, the above results show that RDFP could be a suitable adsorbent since it has the ability to retain its adsorption capability under changing conditions in its surrounding.

3.4. Adsorption isotherm of CR onto RDFP

Adsorption isotherms provide information on the adsorption capability of an adsorbent toward an adsorbate. Adsorption data are imperative especially in trying to determine the suitability of the adsorbent when applied to real wastewater treatment processes. An adsorbent with high adsorption capacity is certainly favored in being more
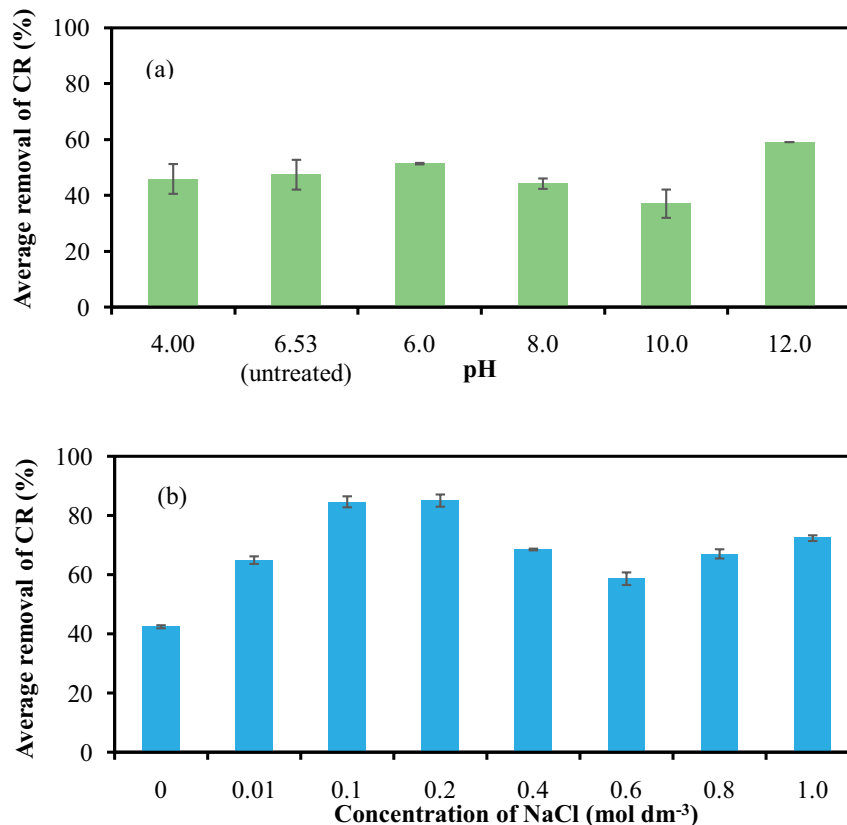

Fig. 4. Effects of (a) pH and (b) ionic strength on the adsorption of CR onto RDFP.

economical and effective in removing unwanted pollutants. In order to understand the adsorption process, different methods of evaluating the experimental equilibrium curves have been reported [44,45]. In this study, the experimental data were fitted to five isotherm models: Langmuir [46], Freundlich [47], Temkin [48], Redlich–Peterson [49] and Sips [50] models, and their nonlinear and linearized equations are shown in Table S1. These isotherm models have been widely discussed and reviewed.

3.4.1. Linear regression analyses

Based on linearized isotherm equations, all the five isotherm models gave high $R^2 > 0.9$, with the Langmuir isotherm showing the highest value followed closely by the Temkin and Sips models. The Freundlich model has the lowest R^2 value. However, it has been reported that linearization could result in bias and change in error structure [51]. In order to avoid these problems, all the isotherm models were subjected to error analyses using five different error functions, namely the average relative error (ARE), sum square errors (SSE), hybrid fractional error function (HYBRID), sum of absolute error (EABS), and chi-square test (c^2), and their equations are outlined in Table S2. The lower the error values, the better fit will be the isotherm model. Of the five isotherm models, the Sips model shows the lowest error values, suggesting that this model be the best fit of all.

Further, the simulation plots of all the five isotherm models as depicted in Fig. 5a show very clearly the deviation of both the Freundlich and Redlich–Peterson models from the experiment data. The Sips and Temkin models, on the other hand, appear reasonably close to the experiment data.

The Akaike information criterion (AIC), developed by Akaike [52], was also performed using Eq. (1):

$$AIC = N \ln\left(SSE \times N^{-1}\right) + 2\left(p + 1\right) \tag{1}$$

where N is the number of observations; p is the number of parameters; and SSE is the sum square errors.

According to AIC, the smaller the AIC value, the better is the fitting. Based on the AIC values, in decreasing order of best fit isotherm model is as follows: Temkin > Sips > Langmuir > Redlich–Peterson > Freundlich. However, the AIC values of Temkin and Sips were very close. Hence, based on the overall smallest errors, close fit of its simulation plot with experiment data, and small AIC value, the adsorption of CR onto RDFP is better fitted to the Sips isotherm model.

3.4.2. Nonlinear regression analyses

Although the linear regression method offers a simple, fast and easy way of determining the best fit model to the experiment data, this method has its downside in
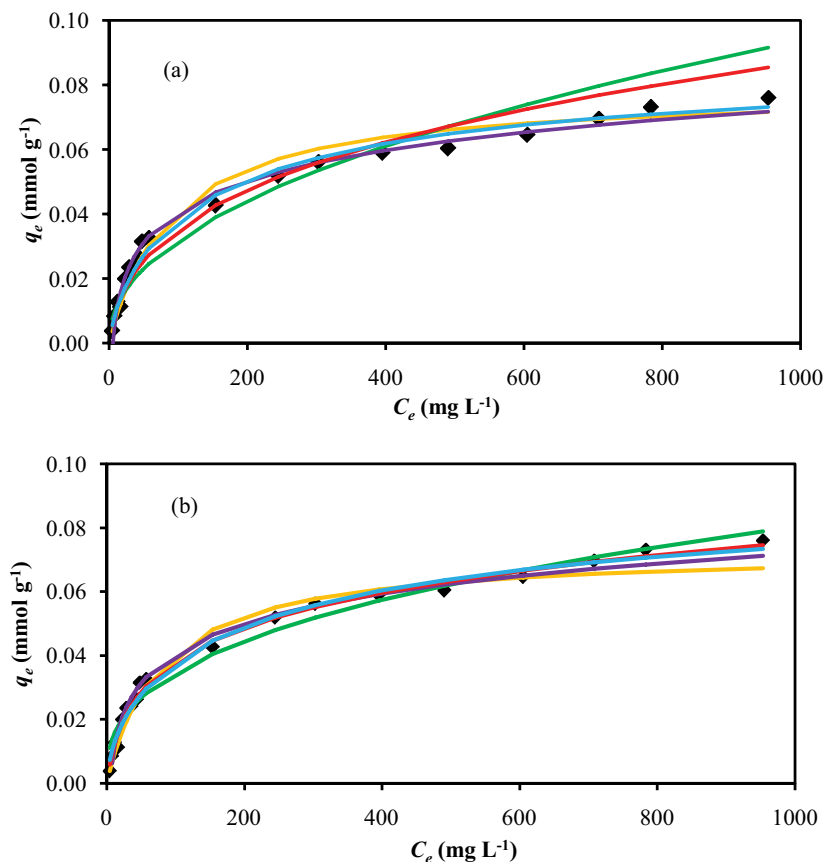

Fig. 5. Comparison of (a) linear and (b) nonlinear regression methods with experiment isotherm data (◆) with Langmuir (——), Freundlich (——), Temkin (——), Redlich–Peterson (——) and Sips (——) models.

that it can lead to errors. The nonlinear regression method generally provides better flexibility in terms of curve fitting and gives lower error values when compared to linear regression [53,54]. Hence, in this study, apart from using the linearized isotherm equations, nonlinear regression method was also employed to analyze experimental data. The R^2 of each model was calculated using Eq. (2):

$$R^2 = \frac{\sum\left(q_{e,\text{cal}} - q_{m,\text{exp}}\right)^2}{\sum\left(q_{e,\text{cal}} - q_{m,\text{exp}}\right)^2 + \left(q_{e,\text{cal}} - q_{m,\text{exp}}\right)^2} \tag{2}$$

where $q_{e,\text{cal}}$ is the calculated amount of adsorbate (mmol g^{-1}); and $q_{m,\text{exp}}$ is the average amount of adsorbate adsorbed from experiment (mmol g^{-1}).

Table 1 shows that of the five isotherm models used, the nonlinear regression indicated that the Freundlich model was the least fitting based on its lowest R^2 and highest error values. Its simulation plot, as shown in Fig. 5b, also deviated from the experimental data. This finding is agreeable to that from the linear regression analyses.

As in the case of linear regression, the Langmuir isotherm has the highest R^2 for nonlinear regression fitting. Even though the Langmuir model gives a better R^2 value than the Redlich–Peterson, error functions show that the latter model has lower overall error values. Nonlinear plots of both the Langmuir and Redlich–Peterson in Fig. 5b also show that the Redlich–Peterson has a closer fit to the experimental data. The nonlinear AIC values, from smallest to highest, are as follows: Redlich–Peterson < Sips < Temkin < Langmuir < Freundlich. When compared between the Langmuir and Sips models, even though the former has a slightly better R^2 value, the Sips model shows a better fit according to Figs. 5 and 6. Error and AIC values also indicate that the Sips model is a better model to describe the adsorption of CR onto RDFP than the Langmuir.

3.4.3. Linear vs. nonlinear regression

Comparison between the linear vs. nonlinear regression of each of the isotherm models is shown in Fig. 6. Of the five isotherm models investigated, only the Temkin and Sips models (Figs. 6c and e, respectively) show close proximity
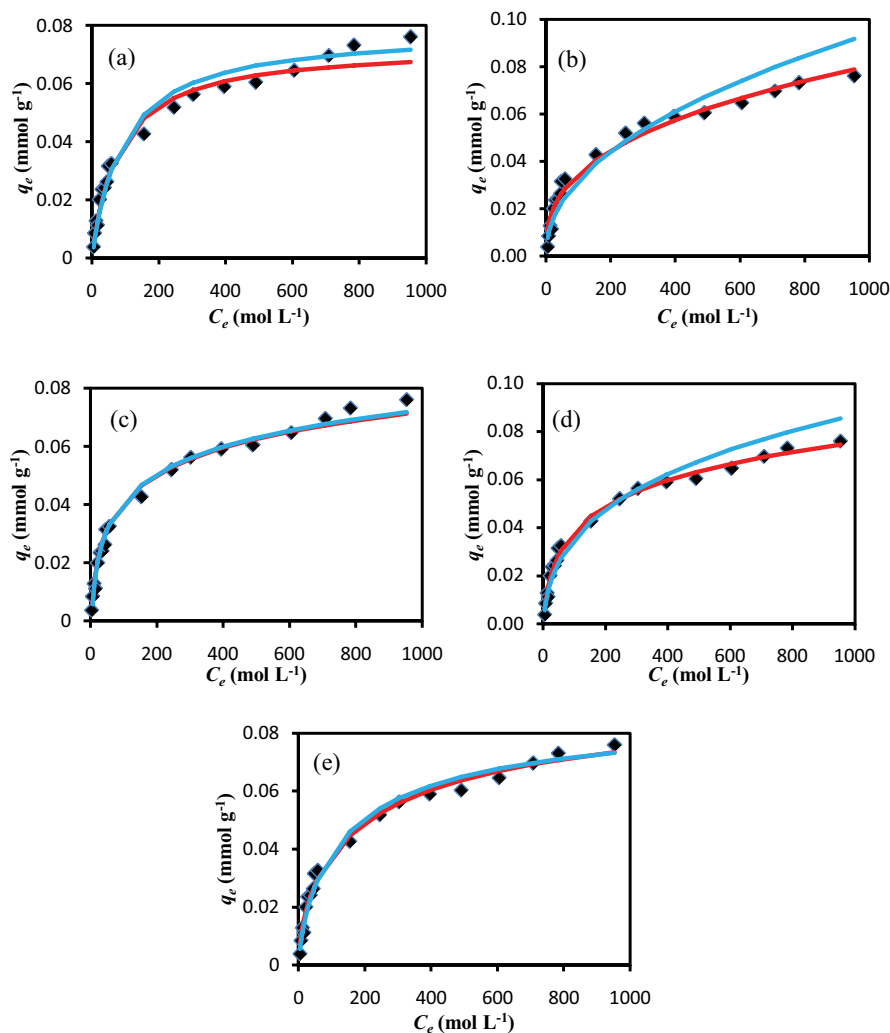

Fig. 6. Comparison of experiment isotherm data (◆) using linear (——) and nonlinear (——) regression methods for (a) Langmuir, (b) Freundlich, (c) Temkin, (d) Redlich–Peterson, and (e) Sips isotherm models.

of both the linear and nonlinear methods. The nonlinear regression method seems to better describe the Freundlich and Redlich–Peterson models than the corresponding linear method, as shown by Figs. 6b and d, respectively. On the other hand, the Langmuir model fits the experimental data slightly better when analyzed using linearized equation. Further, except for Freundlich isotherm, all isotherm models gave lower error values (Table 1) suggesting better accuracy of the nonlinear method.

In order to check if there is any statistically significant difference between the linear and the nonlinear regression methods, ANOVA was used to obtain p-values. According to the null hypothesis, p-value < 0.05 depicts that there is a statistically significant difference while p-value > 0.05 implies there is no significant difference. From Table 2, all the p-values of each isotherm model were >0.05 suggesting that there is no significant difference between the linear and nonlinear regression methods.

3.4.4. Adsorption ability of RDFP

By considering all the above findings, it is recommended that the Sips model be the most appropriate isotherm model, among the five models investigated, to describe the adsorption of CR onto RDFP. Since the nonlinear regression method is more accurate than the corresponding linear method in terms of overall fitting and error values, the maximum adsorption capacity, q_{max}, based on nonlinear regression is 71.74 mg g⁻¹.

In order for an adsorbent to be considered a potential candidate in wastewater treatment, one crucial criterion is in its ability to remove adsorbate efficiently. Therefore, a good q_{max} is indispensable since the adsorbent will be more effective and cost-saving. Table 3 shows a list of some reported adsorbents for the removal of CR dye. RDFP

Table 2
Comparison of linear and nonlinear data obtained for the five isotherm models

Model	Linear	Nonlinear	p-value
Langmuir			0.86
q_{max} (mmol g⁻¹)	0.078	0.073	
q_{max} (mg g⁻¹)	54.617	50.856	
K_L (L mmol⁻¹)	0.011	0.013	
R^2	0.9897	0.9875	
Freundlich			0.95
K_F (mmol g⁻¹ (L mmol⁻¹)$^{1/n}$)	0.004	0.006	
K_F (mg$^{1-1/n}$ L$^{1/n}$ g⁻¹)	2.583	4.484	
n	2.139	2.737	
R^2	0.9188	0.9212	
Temkin			1.00
K_T (L mmol⁻¹)	0.193	0.202	
b_T (kJ mol⁻¹)	180.08	183.00	
R^2	0.9856	0.9545	
Redlich–Peterson			0.91
K_R (L g⁻¹)	0.0019	0.002	
β	0.679	0.794	
$α_R$ (L mmol⁻¹)	0.191	0.091	
R^2	0.9460	0.9760	
Sips			0.97
q_{max} (mmol g⁻¹)	0.090	0.103	
q_{max} (mg g⁻¹)	62.700	71.736	
K_S (L mmol⁻¹)	0.020	0.029	
$1/n$	0.783	0.648	
n	1.277	1.543	
R^2	0.9807	0.9672	

Table 1
Data obtained for the five isotherm models and their error and AIC values

Model	R^2	ARE	SSE	HYBRID	EABS	$χ^2$	AIC
Langmuir							
Linear	0.9897	10.63	0.0003	0.05	0.06	0.02	−205.97
Nonlinear	0.9875	9.29	0.0003	0.04	0.06	0.02	−207.01
Freundlich							
Linear	0.9188	19.45	0.0009	0.13	0.11	0.03	−183.71
Nonlinear	0.9212	21.80	0.0002	0.15	0.05	0.03	−208.01
Temkin							
Linear	0.9856	15.79	0.0001	0.08	0.04	0.03	−217.68
Nonlinear	0.9545	14.73	0.0001	0.07	0.04	0.03	−217.36
Redlich–Peterson							
Linear	0.9460	12.29	0.0004	0.06	0.07	0.02	−195.19
Nonlinear	0.9760	8.46	0.0001	0.03	0.03	0.01	−230.03
Sips							
Linear	0.9807	9.77	0.0001	0.03	0.05	0.02	−216.46
Nonlinear	0.9672	11.85	0.0001	0.05	0.04	0.01	−222.00

Table 3
Comparison of maximum adsorption capacity (q_{max}) of RDFP with selected natural and modified adsorbents

Adsorbent	q_{max} (mg g^{-1})	Reference
Hylocereus polyrhizus (red dragon fruit) peel	71.7	This study
Hylocereus undatus (white dragon fruit) peel	76.6	[39]
Raphanus sativus (radish) peel	0.5	[55]
Tamarind fruit shell	10.5	[56]
Citrus limonum (lemon) peel	34.5	[57]
Cellulosic waste orange peel	22.4	[58]
Banana peel	44.4	[59]
Banana peel	1.7	[60]
Pineapple (*Ananas comosus*) plant stem	12.0	[61]
Watermelon rind	24.8	[62]
Psidium guajava (guava) peel	61.1	[63]
Pomelo fruit peel	1.1	[64]
Pomegranate activated carbon	10.0	[65]
Apricot stone	32.9	[66]
Myrtus communis activated carbon	19.2	[65]
Eichhornia crassipes roots	1.6	[67]
Kaolin	5.4	[68]
Peat	10.1	[69]
Acid activated red mud	7.1	[70]
Jujuba seeds	55.6	[71]
Bagasse charcoal	45.3	[59]
Cattail root	38.8	[72]
Neem leaves	26.1	[62]
Raw pine	32.7	[73]
Acid treated pine	40.2	[73]
Eucalyptus globulus saw dust	5.1	[74]
Phoenix dactylifera (date) seeds	61.7	[75]
Ball-milled sugarcane bagasse	38.2	[76]
Natural pumice	3.9	[77]
Cationic surfactant modified pumice	27.3	[77]
Eggshells	69.5	[78]
Chemically modified eggshell membrane	117.7	[79]
Acid modified celery (*Apium graveolens*)	238.1	[80]
Modified zeolite	69.9	[81]
Exfoliated graphite	80.8	[82]
Chir pine sawdust	5.8	[83]
Pine bark	3.9	[84]

shows similar q_{max} to the peel of white dragon fruit, with the latter being slightly higher in value. When compared to other fruit peels, RDFP shows much higher q_{max}. Similarly, when compared to soil materials and natural adsorbents, the q_{max} obtained for RDFP is promising. Thus, RDFP could have its application as a low-cost adsorbent in wastewater treatment. Further, enhancement of the q_{max} of RDFP through surface modification is a possibility as shown by natural pumice which was chemically treated with acid to improve its adsorption capacity.

3.5. Kinetics of adsorption of CR onto RDFP

Understanding of the adsorption kinetics is vital in wastewater treatment processes as this helps provide information on the cost and design of the adsorption system. In this study, two kinetics models were used namely the Lagergren pseudo-first-order [85] and pseudo-second-order [86]. Their equations are shown as Eqs. (3) and (5), respectively whilst the linearized equations are presented as Eqs. (4) and (6), respectively. These two models have been widely discussed in adsorption studies.
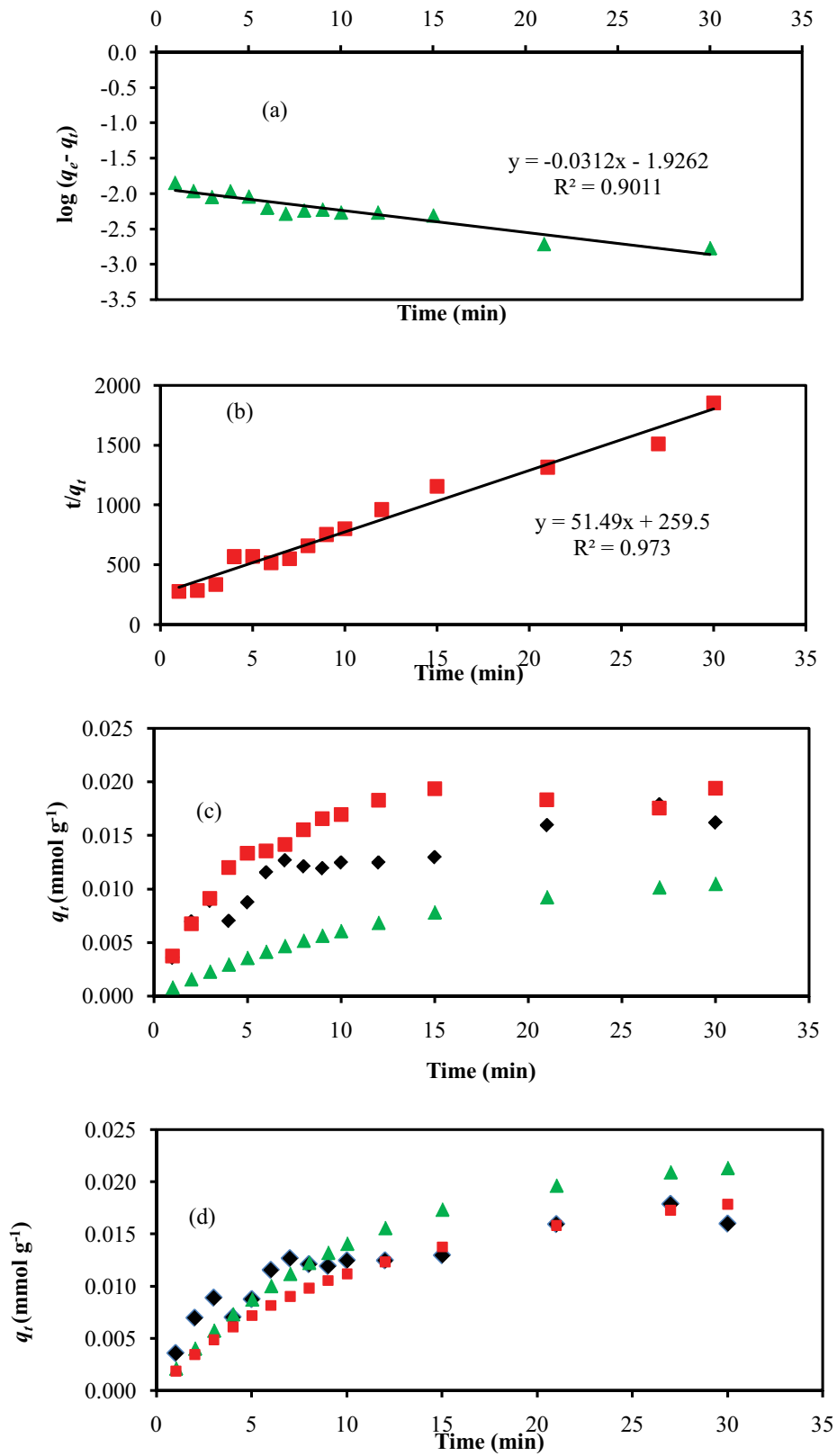
Fig. 7. (a) Linear plot of Lagergren pseudo-first-order kinetics, (b) linear plot of pseudo-second-order kinetics, and comparison of (c) linear and (d) nonlinear regression of experiment data (◆) with the Lagergren pseudo-first-order (▲) and pseudo-second-order (■) models.

Lagergren pseudo-first-order:

$$q_t = q_e \left(1 - e^{-kt}\right) \tag{3}$$

$$\log\left(q_e - q_t\right) = \log\left(q_e\right) - \frac{k_1}{2.303} \tag{4}$$

Pseudo-second-order:

$$q_t = \frac{q^2 e^{kt}}{1 + \left(kq_t t\right)} \tag{5}$$

$$\frac{t}{q_t} = \frac{1}{k_2 q_e^2} + \frac{1}{q_e} \tag{6}$$

where q_t and q_e are adsorption capacity at time t and equilibrium, respectively; k_1 and k_2 are rate constant for pseudo-first-order and pseudo-second-order, respectively.

From the linear plots of the Lagergren pseudo-first-order and pseudo-second-order models as shown in Figs. 7a and b, respectively, both the kinetics models gave good $R^2 > 0.9$. Nevertheless, the pseudo-second-order kinetics has a higher R^2 close to unity (0.9753) compared to pseudo-first-order (0.9011). The overall error values based on six different error analyses, as shown in Table 4, were also much smaller for the pseudo-second-order, thus pointing to this model being the better model to describe the adsorption kinetics of CR onto RDFP. Simulation of the two models as shown in Fig. 7c further confirms that the pseudo-second-order model is much closer to the experiment data.

Nonlinear regression analyses performed on the adsorption kinetics indicate that R^2 obtained from nonlinear regression are very much similar to those from the linear plots (Table 4), with the pseudo-second-order kinetics having R^2 close to unity. The errors of both the linear and nonlinear analyses also showed a clear cut, with the pseudo-second-order kinetic model having much smaller error values than the Lagergren pseudo-first-order

model. Further confirmation is from the AIC value for the pseudo-second-order which was slightly smaller in value.

The nonlinear plots of the two models, as shown in Fig. 7d, both fitted much better to the experimental data than the corresponding linear analyses. Table 4 also shows that their error values were also much smaller than the corresponding linearized method. Thus, it can be concluded that the nonlinear regression method of analysis is a better approach in analyzing the adsorption kinetics of CR onto RDFP.

ANOVA analyses was performed on kinetics data show that the *p*-values for Lagergren first order and pseudo-second-order kinetics are 0.001 and 0.029, respectively. Both *p*-values being <0.05 are indicative that there is statistical significant difference between the two methods used. Nevertheless, combining all the above findings, the pseudo-second-order is the better model to describe the adsorption kinetics of CR onto RDFP.

The adsorption rate of CR onto RDFP is much faster when compared to *Hylocereus undatus*, the white dragon fruit species, with reported k_2 of 1.87 g mmol^{-1} min^{-1} [39].

4. Conclusion

The present study focuses on the use of RDFP as a biosorbent for the removal of Congo red dye from aqueous solution. The adsorbent–adsorbate equilibrated within 30 min of contact time. The Sips adsorption isotherm is the most appropriate model by considering both linear and nonlinear regression methods, error function analyses and ANOVA. The adsorption capacity based on the Sips model is 71.7 mg g^{-1}, which is much higher than that of many fruit peels and other natural adsorbents reported. Adsorption kinetics was best described by the pseudo-second-order model. Using linear and nonlinear regression methods to analyze isotherm and kinetics data, it is found that generally the nonlinear regression is the better method of analyses with closer fit and smaller errors. There were also significant differences between the two regression methods with *p*-values < 0.05 for both the kinetics models, although no

Table 4
Comparison of the Lagergren pseudo-first-order and pseudo-second-order kinetic models using linear and nonlinear regression analyses

Parameter	Linear		Nonlinear	
	Pseudo-first-order	Pseudo-second-order	Pseudo-first-order	Pseudo-second-order
k_1 (min^{-1})	0.0719		0.210	
k_2 (g mmol^{-1} min^{-1})		10.214		11.24
q_{cal} (mmol g^{-1})	0.012	0.020	0.015	0.019
R^2	0.9011	0.9735	0.9066	0.9992
ARE	47.87	23.95	10.533	8.619
HYBRID	0.334	0.128	0.016	0.013
EABS	0.090	0.044	0.018	0.014
χ^2	0.049	0.018	0.003	0.002
SSE	0.0006	0.0002	2.7×10^{-5}	1.8×10^{-5}
AIC	−146.79	−162.79	−191.68	−198.55
q_{exp} (mmol g^{-1})	0.033			

significant difference was observed when applied to the adsorption isotherm data. Overall, RDFP demonstrates its strong ability to withstand changes in both pH and ionic strength while maintaining good adsorption. Being readily available in abundance together with the promising results obtained, RDFP therefore could have potential to be applied in real wastewater treatment as a low-cost adsorbent. Such applications would require a series of optimization steps under both static and dynamic conditions with small-scale, medium-scale and large-scale approaches.

Acknowledgement

References

[1] O. Oyebode, V. Gordon-Dseagu, A. Walker, J.S. Mindell, Fruit and vegetable consumption and all-cause, cancer and CVD mortality: analysis of health survey for England data, J. Epidemiol Community Health, 68 (2014) 856–862.

[2] Y.P. Tang, B.L.L. Linda, L.W. Franz, Proximate analysis of *Artocarpus odoratissimus* (Tarap) in Brunei Darussalam, Int. Food Res. J., 20 (2013) 409–415.

[3] N. Priyantha, L.B.L. Lim, N.H.M. Mansor, A.B. Liyandeniya, Irreversible sorption of Pb(II) from aqueous solution on breadfruit peel to mitigate environmental pollution problems, Water Sci. Technol., 80 (2019) 2241–2249.

[4] Z.M. Yunus, N. Othman, A. Al-Gheethi, R. Hamdan, N.N. Ruslan, Adsorption of heavy metals from mining effluents using honeydew peels activated carbon; isotherm, kinetic and colum studies, J. Dispersion Sci. Technol., (2020) 1–15. https://doi.org/10.1080/01932691.2019.1709493.

[5] L.B.L. Lim, N. Priyantha, M.H.F. Lai, R.M. Salleha, T. Zehra, Utilization of artocarpus hybrid (Nanchem) skin for the removal of Pb(II): equilibrium, thermodynamics, kinetics and regeneration studies, Int. Food Res. J., 22 (2015) 1043–1052.

[6] T.A. Khan, A.A. Mukhlif, E.A. Khan, Uptake of Cu^{2+} and Zn^{2+} from simulated wastewater using muskmelon peel biochar: isotherm and kinetic studies, Egypt. J. Basic Appl. Sci., 4 (2017) 236–248.

[7] L.B.L. Lim, N. Priyantha, X.H. Bong, N.A.H. Mohamad Zaidi, Enhancement of adsorption characteristics of methyl violet 2B dye through NaOH treatment of *Cucumis melo var. cantalupensis* (rock melon) skin, Desal. Water Treat., 18 (2020) 336–348.

[8] M.R.R. Kooh, M.K. Dahri, L.B.L. Lim, Jackfruit seed as low-cost adsorbent for removal of malachite green: artificial neural network and random forest approaches, Environ. Earth Sci., 77 (2018) 434, https://doi.org/10.1007/s12665-018-7618-9.

[9] L.B.L. Lim, N. Priyantha, T. Zehra, C.W. Then, C.M. Chan, Adsorption of crystal violet dye from aqueous solution onto chemically treated *Artocarpus odoratissimus* skin: equilibrium, thermodynamics, and kinetics studies, Desal. Water Treat., 57 (2016) 10246–10260.

[10] T.A. Khan, M. Nazir, E.A. Khan, Adsorptive removal of rhodamine B from textile wastewater using water chestnut (*Trapa natans* L.) peel: adsorption dynamics and kinetic studies, Toxicol. Environ. Chem., 95 (2013) 919–931.

[11] T.A. Khan, R. Rahman, I. Ali, E.A. Khan, A.A. Mukhlif, Removal of malachite green from aqueous solution using waste pea shells as low-cost adsorbent – adsorption isotherms and dynamics, Toxicol. Environ. Chem., 96 (2014) 569–578.

[12] E.A. Khan, Shahjahan, T.A. Khan, Adsorption of methyl red on activated carbon derived from custard apple (*Annona squamosa*) fruit shell: equilibrium isotherm and kinetic studies, J. Mol. Liq., 249 (2018) 1195–1211.

[13] T.A. Khan, R. Rahman, E.A. Khan, Decolorization of bismarck brown R and crystal violet in liquid phase using modified pea peels: non-linear isotherm and kinetics modeling, Model. Earth Syst. Environ., 2 (2016) 141.

[14] W.-S. Choo, W.K. Yong, Antioxidant properties of two species of *Hylocereus* fruits, Adv. Appl. Sci. Res., 2 (2011) 418–425.

[15] V.M. Dembitsky, S. Poovarodom, H. Leontowicz, M. Leontowicz, S. Vearasilp, S. Trakhtenberg, S. Gorinstein, The multiple nutrition properties of some exotic fruits: biological activity and active metabolites, Food Res. Int., 44 (2011) 1671–1701.

[16] S. Priatni, A. Pradita, Stability study of betacyanin extract from red dragon fruit (*Hylocereus polyrhizus*) peels, Procedia Chem., 16 (2015) 438–444.

[17] S. Wichienchot, M. Jatupornpipat, R.A. Rastall, Oligosaccharides of pitaya (Dragon fruit) flesh and their prebiotic properties, Food Chem., 120 (2010) 850–857.

[18] B. Jamilah, Shu, M. Kharidah, M.A. Dzulkifly, A. Noranizan, Physico-chemical characteristics of red pitaya (*Hylocereus polyrhizus*) peel, Int. Food Res. J., 18 (2011) 279–286.

[19] H.Y. Leong, C.W. Ooi, C.L. Law, A.L. Julkifle, G.-T. Pan, P.L. Show, Investigation of betacyanins stability from peel and flesh of red-purple pitaya with food additives supplementation and pH treatments, LWT, 98 (2018) 546–558.

[20] R. Vijayakumar, S.S. Abd Gani, N.F. Mohd Mokhtar, Anti-elastase, anti-collagenase and antimicrobial activities of the underutilized red pitaya peel: an in vitro study for anti-aging applications, Asian J. Pharm. Clin. Res., 10 (2017) 251.

[21] N.A.S. Hernawati, R. Shintawaati, D. Priyandoko, The role of red dragon fruit pee (*Hylocereous polyrhizus*) to improvement blood lipid levels of hyperlipidaemia male mice, J. Phys. Conf. Ser., 1013 (2018) 012167.

[22] N. Priyantha, L.B.L. Lim, M.K. Dahri, D.T.B. Tennakoon, Dragon fruit skin as a potential low-cost biosorbent for the removal of manganese(II) ions, J. Appl. Sci. Environ. Sanit., 8 (2013) 179–188.

[23] A.M. Tanasal, N. La Nafie, P. Taba, Biosorption of Cd(II) ion by dragon fruit peel (*Hylocereus polyrhizus*), J. Akta Kim. Indonesian (Indonesia Chim. Acta)., 8 (2015) 18–30.

[24] R. Mallampati, L. Xuanjun, A. Adin, S. Valiyaveettil, Fruit peels as efficient renewable adsorbents for removal of dissolved heavy metals and dyes from water, ACS Sustainable Chem. Eng., 3 (2015) 1117–1124.

[25] N. Priyantha, L.B.L. Lim, M.K. Dahri, Dragon fruit skin as a potential biosorbent for the removal of Methylene blue dye from aqueous solution, Int. Food Res. J., 22 (2015) 2141–2148.

[26] A.H. Jawad, A.M. Kadhum, Y.S. Ngoh, Applicability of dragon fruit (*Hylocereus polyrhizus*) peels as low-cost biosorbent for adsorption of Methylene blue from aqueous solution: kinetics, equilibrium and thermodynamics studies, Desal. Water Treat., 109 (2018) 231–240.

[27] D.P. Steensma, Historical perspective Congo red out of Africa?, Arch. Pathol. Lab. Med., 125 (2001) 250–252.

[28] E.I. Yakupova, L.G. Bobyleva, I.M. Vikhlyantsev, A.G. Bobylev, Congo red and amyloids: history and relationship, Biosci. Rep., 39 (2019) 1–22.

[29] O. Bashir, M.N. Khan, T.A. Khan, Z. Khan, S.A. AL-Thabaiti, Influence of stabilizing agents on the microstructure of co-nanoparticles for removal of Congo red, Environ. Technol. Innovation, 8 (2017) 327–342.

[30] M.N. Khan, O. Bashir, T.A. Khan, S.A. Al-Thabaiti, Z. Khan, Catalytic activity of cobalt nanoparticles for dye and 4-nitro phenol degradation: a kinetic and mechanistic study, Int. J. Chem. Kinet., 49 (2017) 438–454.

[31] O. Hörstensmeyer, Tödlicher Zwischenfall nach intravenöser Injektion von Kongorot, DMW – Dtsch. Medizinische Wochenschrift, 89 (1964) 1845–1848.

[32] C. Schilliger-Musset, Inclusion of Substances of Very High Concern in the Candidate List for Eventual Inclusion in Annex XIV, Decision of the European Chemicals Agency, ECHA European Chemicals Agency, ED/121/2013, 2013, pp. 1–5.

[33] X.-Y. You, J.-G. Chen, Y.-N. Hu, Studies on the relation between bladder cancer and benzidine or its derived dyes in Shanghai, Br. J. Ind. Med., 47 (1990) 544–552.

[34] L.E. Gray, J.S. Ostby, The effects of prenatal administration of azo dyes on testicular development in the mouse: a structure activity profile of dyes derived from benzidine, dimethylbenzidine, or dimethoxybenzidine, Toxicol. Sci., 20 (1993) 177–183.

[35] V.R.N. Nethi, Biosorption and optimization studies on Congo red dye with fanwort powder using box behnken design, Int. Res. J. Eng. Technol., 5 (2018) 728–738.

[36] R. De, H. Lee, B. Das, Exploring the interactions in binary mixtures of polyelectrolytes: influence of mixture composition, concentration, and temperature on counterion condensation, J. Mol. Liq., 251 (2018) 94–99.

[37] S.A. Moon, B.K. Salunke, P. Saha, A.R. Deshmukh, B.S. Kim, Comparison of dye degradation potential of biosynthesized copper oxide, manganese dioxide, and silver nanoparticles using kalopanax pictus plant extract, Korean J. Chem. Eng., 35 (2018) 702–708.

[38] A. Bartošová, L. Blinová, M. Sirotiak, A. Michalíková, Usage of FTIR-ATR as non-destructive analysis of selected toxic dyes, Sciendo, 25 (2017) 103–111.

[39] L.B.L. Lim, N. Priyantha, S.A. Abdul Latip, Y.C. Lu, A.H. Mahadi, Converting *Hylocereus undatus* (white dragon fruit) peel waste into a useful potential adsorbent for the removal of toxic Congo red dye, Desal. Water Treat., 185 (2020) 307–317.

[40] M. Bergaoui, A. Nakhli, Y. Benguerba, M. Khalfaoui, A. Erto, F.E. Soetaredjo, S. Ismadji, B. Ernst, Novel insights into the adsorption mechanism of Methylene blue onto organo-bentonite: adsorption isotherms modeling and molecular simulation, J. Mol. Liq., 272 (2018) 697–707.

[41] Y.C. Lu, N. Priyantha, L.B.L. Lim, *Ipomoea aquatica* roots as environmentally friendly and green adsorbent for efficient removal of Auramine O dye, Surf. Interfaces, 20 (2020) 100543.

[42] A.A. Romzi, L.B.L. Lim, C.M. Chan, N. Priyantha, Application of *Dimocarpus longan* ssp. *malesianus* leaves in the sequestration of toxic brilliant green dye, Desal. Water Treat., 189 (2020) 428–439.

[43] M.K. Dahri, L.B.L. Lim, C.C. Mei, Cempedak durian as a potential biosorbent for the removal of brilliant green dye from aqueous solution: equilibrium, thermodynamics and kinetics studies, Environ. Monit. Assess., 187 (2015) 546, https://doi.org/10.1007/s10661-015-4768-z.

[44] G.L. Dotto, L.A.A. Pinto, M.A. Hachicha, S. Knani, New physicochemical interpretations for the adsorption of food dyes on chitosan films using statistical physics treatment, Food Chem., 171 (2015) 1–7.

[45] L. Sellaoui, H. Guedidi, S. Knani, L. Reinert, L. Duclaux, A.B. Lamine, Application of statistical physics formalism to the modeling of adsorption isotherms of ibuprofen on activated carbon, Fluid Phase Equilib., 387 (2015) 103–110.

[46] I. Langmuir, The adsorption of gases on plane surfaces of glass, mica and platinum, J. Am. Chem. Soc., 40 (1918) 1361–1403.

[47] H. Freundlich, Over the adsorption in the solution, J. Phys. Chem., 57 (1906) 385–470.

[48] M.J. Temkin, V. Pyzhev, Kinetics of ammonia synthesis on promoted iron catalysts, Acta Physiochim., 12 (1940) 217.

[49] O. Redlich, D.L. Peterson, A useful adsorption isotherm, J. Phys. Chem., 63 (1959) 1024.

[50] R. Sips, On the structure of a catalyst surface, J. Chem. Phys., 16 (1948) 490–495.

[51] K.V. Kumar, Comparative analysis of linear and non-linear method of estimating the sorption isotherm parameters for malachite green onto activated carbon, J. Hazard. Mater., 136 (2006) 197–202.

[52] H. Akaike, A new look at the statistical model identification, IEEE Tans. Autom. Control., 19 (1974) 716–723.

[53] H.R. Ghaffari, H. Pasalari, A. Tajvar, K. Dindarloo, B. Bak-Goudarzi, V. Alipour, A. Ghanbarneajd, Linear and nonlinear two-parameter adsorption isotherm modeling: a case-study, Int. J. Eng. Sci., 6 (2017) 1–11.

[54] M. Yadav, N.K. Singh, Isotherm investigation for the sorption of fluoride onto Bio-F: comparison of linear and non-linear regression method, Appl. Water Sci., 7 (2017) 4793–4800.

[55] A. Abbas, S. Murtaza, M. Munir, T. Zahid, N. Abbas, A. Mushtaq, Removal of Congo red from aqueous solutions with *Raphanus sativus* peels and activated carbon: a comparative study, American-Eurasian J. Agri. Envir. Sci., 10 (2011) 802–809.

[56] S. Reddy, Removal of direct dye from aqueous solutions with an adsorbent made from tamarind fruit shell, an agricultural solid waste, J. Sci. Ind. Res., 65 (2006) 443–446.

[57] A. Bhatnagar, E. Kumar, A.K. Minocha, B.H. Jeon, H. Song, Y.C. Seo, Removal of anionic dyes from water using *Citrus limonum* (Lemon) peel: equilibrium studies and kinetic modeling, Sep. Sci. Technol., 44 (2009) 316–334.

[58] C. Namasivayam, N. Muniasamy, K. Gayatri, M. Rani, K. Ranganathan, Removal of dyes from aqueous solutions by cellulosic waste orange peel, Bioresour. Technol., 57 (1996) 37–43.

[59] Sumanjit, S. Rani, R.K. Mahajan, Kinetic and equilibrium studies of adsorption of dye Congo red from aqueous solutions on bagasse charcoal and banana peels, J. Surf. Sci. Technol., 28 (2012) 133–147.

[60] N.K. Mondal, S. Kar, Potentiality of banana peel for removal of Congo red dye from aqueous solution: isotherm, kinetics and thermodynamics studies, Appl. Water Sci., 8 (2018) 157.

[61] S.L. Chan, Y.P. Tan, A.H. Abdullah, S.T. Ong, Equilibrium, kinetic and thermodynamic studies of a new potential biosorbent for the removal of basic blue 3 and Congo red dyes: pineapple (*Ananas comosus*) plant stem, J. Taiwan Inst. Chem. Eng., 61 (2016) 306–315.

[62] M.B. Sani, Comparative isotherms studies on adsorptive removal of Congo red from wastewater by watermelon rinds and neem-tree leaves, Open J. Phys. Chem., 4 (2014) 139–146.

[63] P. Singh, P. Raizada, D. Pathania, G. Sharma, P. Sharma, Microwave induced KOH activation of guava peel carbon as an adsorbent for Congo red dye removal from aqueous phase, Indian J. Chem. Technol., 20 (2013) 305–311.

[64] M. Jayarajan, R. Arunachala, G. Annadurai, Use of low cost nano-porous materials of pomelo fruit peel wastes in removal of textile dye, Res. J. Environ. Sci., 5 (2011) 434–443.

[65] M. Ghaedi, H. Tavallali, M. Sharifi, S.N. Kokhdan, A. Asghari, Preparation of low cost activated carbon from *Myrtus communis* and pomegranate and their efficient application for removal of Congo red from aqueous solution, Spectrochim. Acta, Part A, 86 (2012) 107–114.

[66] M. Abbas, M. Trari, Kinetic, equilibrium and thermodynamic study on the removal of Congo red from aqueous solutions by adsorption onto apricot stone, Process Saf. Environ. Prot., 98 (2015) 424–436.

[67] W.C. Wanyonyi, J.M. Onyari, P.M. Shiundu, Adsorption of Congo red dye from aqueous solutions using roots of *Eichhornia crassipes*: kinetic and equilibrium studies, Energy Procedia, 50 (2014) 862–869.

[68] V. Vimonses, S. Lei, B. Jin, C.W.K. Chow, C. Saint, Kinetic study and equilibrium isotherm analysis of Congo red adsorption by clay materials, Chem. Eng. J., 148 (2009) 354–364.

[69] T. Zehra, N. Priyantha, L.B.L. Lim, E. Iqbal, Sorption characteristics of peat of Brunei Darussalam V: removal of Congo red dye from aqueous solution by peat, Desal. Water Treat., 54 (2015) 2592–2600.

[70] A. Tor, Y. Cengeloglu, Removal of Congo red from aqueous solution by adsorption onto acid activated red mud., J. Hazard. Mater., 138 (2006) 409–415.

[71] M.C.S. Reddy, L. Sivaramakrishna, A.V. Reddy, The use of an agricultural waste material, jujuba seeds for the removal of anionic dye (Congo red) from aqueous medium, J. Hazard. Mater., 203–204 (2012) 118–127.

[72] Z. Hu, H. Chen, F. Ji, S. Yuan, Removal of Congo red from aqueous solution by cattail root, J. Hazard. Mater., 173 (2010) 292–297.

[73] S. Dawood, T.K. Sen, Removal of anionic dye Congo red from aqueous solution by raw pine and acid-treated pine cone

powder as adsorbent: equilibrium, thermodynamic, kinetics, mechanism and process design, Water Res., 46 (2012) 1933–1946.

[74] V.S. Mane, P.V. Vijay Babu, Kinetic and equilibrium studies on the removal of Congo red from aqueous solution using eucalyptus wood (*Eucalyptus globulus*) saw dust, J. Taiwan Inst. Chem. Eng., 44 (2013) 81–88.

[75] D. Pathania, A. Sharma, Z.M. Siddiqi, Removal of Congo red dye from aqueous system using *Phoenix dactylifera* seeds, J. Mol. Liq., 219 (2016) 359–367.

[76] Z. Zhang, L. Moghaddam, I.M. O'Hara, W.O.S. Doherty, Congo red adsorption by ball-milled sugarcane bagasse, Chem. Eng. J., 178 (2011) 122–128.

[77] H. Shayesteh, A. Rahbar-Kelishami, R. Norouzbeigi, Evaluation of natural and cationic surfactant modified pumice for Congo red removal in batch mode: kinetic, equilibrium, and thermodynamic studies, J. Mol. Liq., 221 (2016) 1–11.

[78] P.D. Saha, S. Chowdhury, M. Mondal, K. Sinha, Biosorption of direct red 28 (Congo red) from aqueous solutions by eggshells: batch and column studies, Sep. Sci. Technol., 47 (2012) 112–123.

[79] S. Parvin, B.K. Biswas, M.A. Rahman, M.H. Rahman, M.S. Anik, M.R. Uddin, Study on adsorption of Congo red onto chemically modified egg shell membrane, Chemosphere, 236 (2019) 124326.

[80] S. Mohebali, D. Bastani, H. Shayesteh, Equilibrium, kinetic and thermodynamic studies of a low-cost biosorbent for the removal of Congo red dye: acid and CTAB-acid modified celery (*Apium graveolens*), J. Mol. Struct., 1176 (2019) 181–193.

[81] S. Liu, Y. Ding, P. Li, K. Diao, X. Tan, F. Lei, Y. Zhan, Q. Li, B. Huang, Z. Huang, Adsorption of the anionic dye Congo red from aqueous solution onto natural zeolites modified with N,N-dimethyl dehydroabietylamine oxide, Chem. Eng. J., 248 (2014) 135–144.

[82] T.V. Pham, T.V. Tran, T.D. Nguyen, N.T.H. Tham, P.T.T. Quang, D.T.T. Uyen, N.T.H. Le, D.-V.N. Vo, N.T. Thanh, L.G. Bach, Adsorption behavior of Congo red dye from aqueous solutions onto exfoliated graphite as an adsorbent: kinetic and isotherm studies, Mater. today:. Proc., 18 (2019) 4449–4457.

[83] T.A. Khan, S. Sharma, E.A. Khan, A.A. Mukhlif, Removal of Congo red and basic violet 1 by chir pine (Pinus roxburghii) sawdust, a saw mill waste: batch and column studies, Toxicol. Environ. Chem., 96 (2014) 555–568.

[84] K. Litefti, M.S. Freire, M. Stitou, J. González-Álvarez, Adsorption of an anionic dye (Congo red) from aqueous solutions by pine bark, Sci. Rep., 9 (2019) 16530.

[85] S. Lagergren, About the theory of so-called adsorption of soluble substances, K. Sven. Vetenskapsakad. Handl., 24 (1898) 1–39.

[86] Y.S. Ho, G. McKay, Sorption of dye from aqueous solution by peat, Chem. Eng. J., 70 (1998) 115–124.
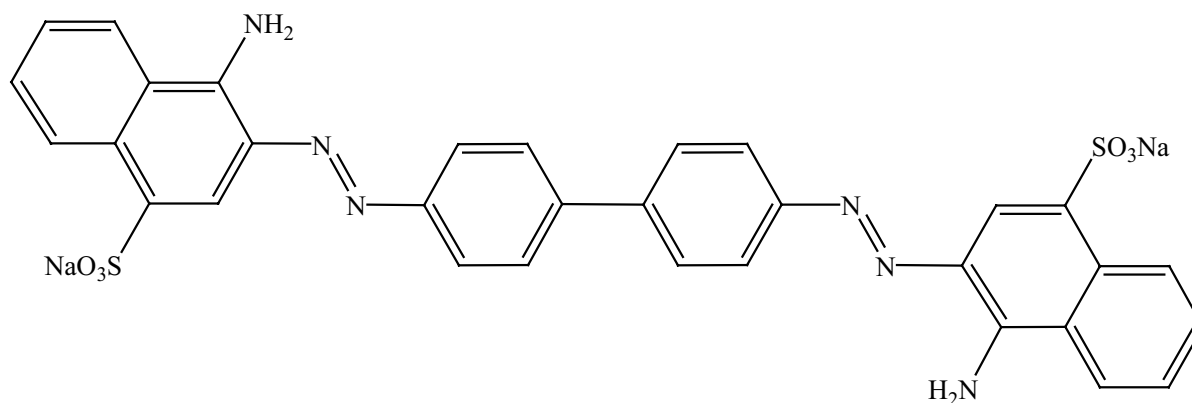
Supplementary information

Fig. S1. Structure of Congo red dye.

Table S1
Isotherm models used in this study

Equations	
Nonlinear isotherm models	Linearized isotherm models

Langmuir

$$q_e = \frac{Q_m K_L C_e}{1 + K_L C_e}$$

Langmuir

$$\frac{C_e}{q_e} = \frac{1}{K_L q_{max}} + \frac{C_e}{q_{max}}$$

Freundlich

$$q_e = K_F C_e^{\frac{1}{n}}$$

Freundlich

$$\log q_e = \frac{1}{n} \log C_e + \log K_F$$

Temkin

$$q_e = \frac{RT \ln(K_T C_e)}{b_T}$$

Temkin

$$q_e = \left(\frac{RT}{b_T}\right) \ln K_T + \left(\frac{RT}{b_T}\right) \ln C_e$$

Redlich–Peterson

$$q_e = \frac{K_R C_e}{1 + \alpha_R C_e^{\beta}}$$

Redlich–Peterson

$$\ln\left(\frac{K_R C_e}{q_e} - 1\right) = \beta \ln C_e + \ln \alpha_R$$

Sips

$$q_e = \frac{q_m K_s C_e^{\frac{1}{n}}}{1 + K_s C_e^{\frac{1}{n}}}$$

Sips

$$\ln\left(\frac{q_e}{q_{max} - q_e}\right) = \frac{1}{n} \ln C_e + \ln K_s$$

K_L and K_F are the Langmuir constant (L mmol^{-1}) and the Freundlich adsorption capacity constant (mmol g^{-1} (L mmol^{-1})$^{1/n}$), respectively; where n indicates how favorable the adsorption intensity on the heterogeneous surface; K_T is the Temkin isotherm constant (L mmol^{-1}); b_T is related to the heat of adsorption (J mol^{-1}); whilst R is the gas constant (J K^{-1} mol^{-1}); T is the room temperature (K); K_R, α_R and β are the Redlich–Peterson isotherm constant (L g^{-1}), Redlich–Peterson constant (L mmol^{-1}), and exponent between 0 and 1, respectively; K_s and n are the Sips isotherm constant (L mmol^{-1}) and dimensionless heterogeneity factor, respectively; q_e is the adsorption capacity at equilibrium; q_{max} is the maximum adsorption capacity; C_e is the equilibrium concentration (mg L^{-1}).

Table S2
Error functions used in this study

Error functions and their equations

ARE

$$\frac{100}{n} \sum_{i=1}^{n} \left| \frac{q_e - q_{e,cal}}{q_{e,meas}} \right|_i$$

SSE

$$\sum_{i=1}^{n} \left(q_{e,cal} - q_e \right)_i^2$$

HYBRID

$$\frac{100}{n-p} \sum_{i=1}^{n} \left| \frac{\left(q_e - q_{e,cal}\right)^2}{q_{e,meas}} \right|_i$$

EABS

$$\sum_{i=1}^{n} \left| q_e - q_{e,cal} \right|$$

χ^2

$$\sum_{i=1}^{n} \frac{\left(q_e - q_{e,cal} \right)^2}{q_e}$$

q_e and $q_{e,cal}$ are the equilibrium and calculated adsorption capacity, respectively; n is the number of data in the experiment.